Separation and mechanical properties of residual film and soil

Yu Ren[1,2], Wensong Guo[1,2*], Xufeng Wang[1,2], Can Hu[1,2], Long Wang[1,2], Xiaowei He[1,2], Jianfei Xing[1,2]

(1. *College of Mechanical and Electrical Engineering, Tarim University, Alar 843300, Xinjiang, China*;
2. Modern Agricultural Engineering Key Laboratory at Universities of Education Department of Xinjiang Uygur Autonomous Region, Tarim University, Alar 843300, Xinjiang, China)

Abstract: In Xinjiang's perennial cotton (*Gossypium hirsutum*)-planting soil, the average residual amount of plastic film is as high as 265.3 kg/hm^2, and the problem of pollution with residual plastic film in the tillage layer has become a major problem. To explore the mechanism of the separation of residual film and soil in the tillage layer and determine the conditions favorable for the separation of residual film-soil, this study established a constitutive model of residual film-soil contact based on the discrete element method and used the established constitutive model to simulate the process of separating residual film and soil. In addition, the influence of parameters, such as soil particle size and water content, on the force to separate the residual film and soil was studied using single factor and orthogonal experiments. The simulation results showed that the changing trend of the residual film-soil separation force curve did not differ much between the simulation and the actual comparison, and the curves were roughly the same. They all decreased after the separation force reached its peak value, but the simulated separation force curve was similar to that of the actual separation force. It increased rapidly from the beginning and reached peak separation force first. The single-factor experiment showed that the separation force of the used residual mulching film was higher than that of the unused mulching film. Under the same conditions, the maximum separation force required to separate the residual membrane was proportional to the positive pressure on the surface of the residual membrane and the size of soil particles. Under the same conditions, the maximum separation force required to separate the residual film is proportional to the positive pressure on the surface of the residual film and the size of soil particles. The maximum separation force decreased first and then increased as the soil moisture content increased. The results of the orthogonal experiment showed that the soil particle size had the greatest effect on the maximum separation force, followed by positive pressure on the residual film surface, soil moisture content, and the service life of mulch. In addition, film mulch that was buried 60 mm deep in the soil, a particle size of more than 2.5 mm, and a soil moisture content of 8% was the optimal combination of parameters to effectively separate the film mulching residue from the soil.

Keywords: residual mulching film, soil, separation, discrete element simulation, sandy soil
DOI: 10.25165/j.ijabe.20231601.7688

Citation: Ren Y, Guo W S, Wang X F, Hu C, Wang L, He X W, et al. Separation and mechanical properties of residual film and soil. Int J Agric & Biol Eng, 2023; 16(1): 184–192.

1 Introduction

Xinjiang is the largest cotton (*Gossypium hirsutum*)-producing region in China. This was shown by its contribution of more than 80% of China's cotton production for five consecutive years according to the Chinese National Bureau of Statistics[1,2]. The plastic film mulching technique has been widely used to plant cotton in Xinjiang and has significantly increased cotton yields, which has significantly benefitted agricultural production in China and the income of farmers in Xinjiang[3-5]. With the continuous increase in mulching film use and low recovery rate, the residual mulch film (RMF) in the soil gradually increases, which causes serious damage to the soil structure and a gradual deterioration in the quality of cultivated land[6-11]. According to He et al.[12], the average residual amount of mulching film in the topsoil of perennial cotton planting in Xinjiang reached 265.3 kg/hm^2. Currently, RMF pollution has become a serious problem in Xinjiang areas[13-16].

RMF affects not only soil microbial activities and water, air, and mineral transport in the soil but also seed germination and development. Xu et al.[17-21] found that the RMF could inhibit the elongation of the root system, and it had a significant effect on the composition of soil organic matter and the movement of nutrients in the soil; thus, it will destroy the soil structure. Therefore, there is an urgent need to control RMF pollution in farmland.

To remove the RMF from agricultural topsoil, many researchers in China and throughout the world have designed numerous types of machines to recover the residual film. However, the removal rate is low. The reason for this is the lack of research on the mechanical properties of soil that contains residual film. In recent years, many researchers have studied the static and dynamic behavior of soil using the discrete element method (DEM). The DEM has become a very reliable method to study soil behavior[22].

An RMF is a flexible object with a thickness of 0.01 mm. Some researchers have conducted studies to model flexible objects. Lobo-Guerrero et al.[23] used the particle clustering method to study

Received date: 2022-05-19 **Accepted date:** 2022-10-19
Biographies: Yu Ren, Master, research interest: intelligent agricultural equipment, Email: 10757212255@stumail.taru.edu.cn; **Xufeng Wang**, PhD, Professor, research interest: agricultural equipment, Email: wxf@taru.edu.cn; **Can Hu**, PhD, research interest: intelligent agricultural equipment, Email: 120140004@taru.edu.cn; **Long Wang**, PhD candidate, research interest: soil machinery, Email: 120140002@taru.edu.cn; **Xiaowei He**, PhD, research interest: agricultural equipment, Email: 120140001@taru.edu.cn; **Jianfei Xing**, Lecturer, research interest: agricultural equipment, Email: 120200012@taru.edu.cn.
***Corresponding author: Wensong Guo**, PhD, research interest: intelligent agricultural equipment. Mailing address: College of Engineering, Tarim University, 843300, Alar, Xinjiang, China. Tel: +86-18399578707, Email: 120120004@taru.edu.cn.

the strength of soils reinforced by fiber. The disadvantage of this method is the introduction of artificial roughness on the contact surface between the flexible object and the particles. Later, the coupled discrete element methods (DEM) and finite element methods (FEM) were widely adopted; these methods entail modeling flexible structures as finite elements, and granular materials were modeled as discrete spherical particles[24]. This method combines the advantages of DEM and FEM, but it is difficult to accurately define the contact behavior between discrete particles and finite elements[25,26]. Effeindzourou et al.[27,28] used the Minkowski sum method to model the discrete elements of geotextiles and conducted experiments on pulling geotextiles out of the soil.

However, the current studies rarely involve establishing the discrete element model of RMF-soil, and our understanding of the mechanism of separation between RMF-soil is not clear enough. To further study the contact behavior and mechanism of separation between RMF-soil, the discrete element model and separation simulation model of RMF-soil were first established using the discrete element method, and the separation mechanism between RMF-soil was then studied by single factor and orthogonal experimental methods. This study provided a reference for other researchers to study the mechanical properties of RMF-soil separation, which will help to treat RMF pollution.

2 Materials and methods

2.1 Soil and RMF sampling and analysis

2.1.1 Soil sampling and parameter measurement

1) Soil sampling method

The soil samples in this paper were collected from sandy soil in Xinjiang, and the sampling site was the farm of Alar City, Xinjiang Uygur Autonomous Region, China (40°54′N, 81°06′E). The five-point sampling method was used to create quadrats as a square quadrat of 1 m×1 m. The sampling tool was a ring-knife soil borrow drill (QTZ-1, Cangzhou Luyi Testing Instrument Co., Ltd., China). The sampling work was completed within 2 d, and the soil samples obtained were stored in Ziplock bags.

2) Soil basic parameters

The basic characteristics of the 0.00-0.30 m layer of soil that was measured are listed in Table 1.

Table 1 Measured basic properties of 0.00-0.30 m layer of soil in this study

Soil particle density /kg·m^{-3}	Bulk density /kg·m^{-3}	Soil moisture Content/%	Intra–particle friction factor	Shear modulus of elasticity	Group cohesiveness	Poisson ratio
2400-2800	2100-2500	6-26	0.31-0.56	2.1×10^{7}-2.7×10^{7}	1.25×10^{5}-1.85×10^{5}	0.23-0.44

3) Soil particle size distribution

The sieving method was used in this study[29]. The sieving instrument was a standard inspection sieve (GB/T6003.1-2012; Shaoxing Shangyu Huafeng Hardware Instrument Co., Ltd., Zhejiang, China). The apertures were 0.2 mm, 0.6 mm, 1.0 mm, 1.6 mm, 2.0 mm, and 2.5 mm. This study used an electronic balance with an accuracy of 0.001 g. The results of the particle size distribution of the sandy soil obtained are shown in Figure 1.

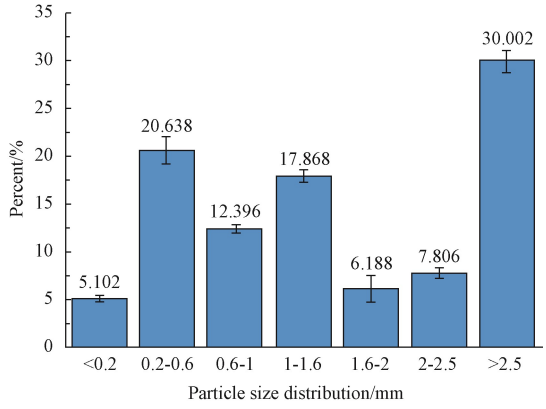

Figure 1 Particle size distribution of sandy soil

4) Soil particle stacking angle

In this experiment, the static-stack angle when the bottom plane remains static was adopted[30]. The stacking angles of soil particles with particle sizes >2.5 mm, 2.0-2.5 mm, 1.6-2.0 mm, 1.0-1.6 mm, 0.6-1.0 mm, 0.2-0.6 mm, <0.2 mm, and unscreened soil were studied. The measurement results are shown in Figure 2. The results showed a decrease in the stacking angle of soil particles, followed by an increase, with a decrease in the particle diameter. In addition, the stacking angle of unscreened soil was 53.73°.

2.1.2 RMF sampling and parameter measurement

1) Sampling of RMF

The mulch film of the experiment material includes unused film and used RMF. The unused mulch film was produced by Yihang Plastic Products Factory, Aksu City, Xinjiang Uygur Autonomous Region. The RMF was collected from land that was covered with film for 5 a. The thickness of all the recovered RMF samples was 0.01 mm, and the RMF that was recovered was stored in Ziplock bags.

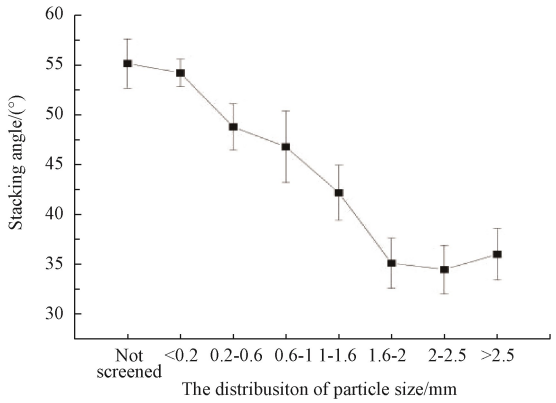

Figure 2 Relationship between soil particle accumulation angle and particle size

2) Basic physical performance parameters of RMF

The physical properties of RMF are listed in Table 2.

Table 2 Basic physical performance parameters of the residual membrane

Mulch type/stretch results	Tensile strength/MPa	Elongation at break/%	Elastic modulus/MPa
Unused film	12.00	3.14	34.40
Used RMF	7.60	1.00	28.10

2.2 RMF-soil separation simulation method

2.2.1 Construction of RMF-soil particle contact constitutive model

The RMF is a highly flexible thin film that performs similarly

to geotextiles. This article refers to the discrete element model of contact between the geotextile and soil established by Effeindzourou et al.[27,28] Yade[31] is an extensible open-source framework for discrete numerical models, which focuses on the discrete element method. The contact constitutive model of RMF and soil was constructed using Yade discrete element software. The specific construction method was as follows:

In this study, the soil particles are considered to be equivalent to spherical particles. The basic primitives of the simulation RMF model constructed based on the Minkowski sum principle include a sphere, cylinder element, and triangular surface element; the cylinder and triangular surface are deformable bodies[32-36]. Arbitrary shape RMF can be constructed by connecting multiple triangular face elements. Therefore, this paper attempted to splice the RMF model from triangular surface elements, which demonstrated that the contact between soil and the RMF primarily occurs between spherical particles and triangular plane elements. Figure 3 shows the contact between RMF and soil particles. A virtual ball was added at the contact position (P). Thus, the contact between the spherical particles and the plane elements was transformed into contact between the spherical particles and the virtual spherical particles. The concept of the virtual ball was introduced to process the ball-plane contact, with P' representing the center of virtual ball. The virtual ball and plane elements have the same material properties, while the diameter of the virtual ball is the same as the thickness of the virtual RMF.

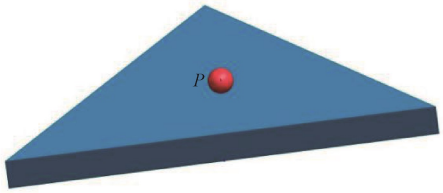

a. Sphere-triangle face element contact

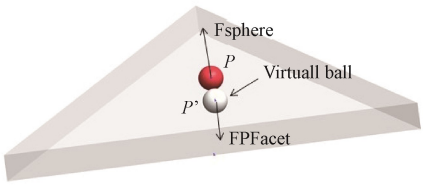

b. Virtual ball contact

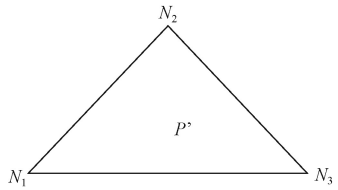

c. Sphere-triangular face plan view

Note: N_1, N_2, and N_3 denote the three nodes of the triangular planar element; P denotes the contact point of the ball plane; P' denotes the center of the virtual ball; F denotes the contact force between soil particles and RMF. RMF, residual mulch film.

Figure 3 Sphere-triangle face element contact, virtual ball contact and sphere-triangular face plan view

The general discrete element contact rule was considered to be the contact rule between spherical particles and virtual spherical particles[37]. The contact force of the virtual ball was distributed to each node of the element based on the position of the contact point. This method is the fundamental calculation of the ball-surface element contact.

For ball-plane contact, the position of contact point P was defined according to three nodes of the triangular planar element and the ball, while P' was projected by the contact point P onto the planar element. The centroid coordinates of P' were p_1, p_2, and p_3. The calculations of the centroid coordinates are expressed in Equations (1)-(3).

$$p_1 = \frac{\|N_1N_3\|(N_1N_2 \cdot N_1P') - (N_1N_2 \cdot N_1N_3)(N_1N_3 \cdot N_1P')}{\|N_1N_2\|\|N_1N_3\| - (N_1N_2 \cdot N_1N_3)(N_1N_2 \cdot N_1)} \quad (1)$$

$$p_2 = \frac{\|N_1N_2\|(N_1N_3 \cdot N_1P') - (N_1N_2 \cdot N_1N_3)(N_1N_2 \cdot N_1P')}{\|N_1N_2\|\|N_1N_3\| - (N_1N_2 \cdot N_1N_3)(N_1N_2 \cdot N_1N_3)} \quad (2)$$

$$p_3 = 1 - p_1 - p_2 \quad (3)$$

The projected position P' was used to define contact between the spherical particle and the triangular plane element. The movement and rotation of the virtual ball were linearly interpolated at the three nodes of N_1, N_2, and N_3 on the plane. The movement velocity v'_p and rotation velocity were calculated using velocities and rotation velocities of three nodes (v_{N1},v_{N2}, and v_{N3}) and (w_{N1}, w_{N2}, and w_{N3}), according to Equations (4) and (5), respectively.

$$v'_p = p_1v_{N_1} + p_2v_{N_2} + p_3v_{N_3} \quad (4)$$

$$w'_p = p_1w_{N_1} + p_2w_{N_2} + p_3W_{N_3} \quad (5)$$

F_{Ni} denotes the force exerted on the node with N_i, $i \in \{1, 2, 3\}$ calculated as described in Equation (6).

$$\begin{cases} F_{N_1} = P_1F \\ F_{N_2} = P_2F \\ F_{N_3} = P_3F \end{cases} \quad (6)$$

2.2.2 Simulation of experimental steps of the separation of RMF from soil

First, a closed square box with length L, width W, and height H of 0.10 m, 0.10 m, and 0.08 m, respectively, was established (Figure 4a). The box consisted of 12 triangular plane elements. All degrees of freedom of movement and rotation of the box were fixed. As for the material properties of the box, Young's modulus, Poisson's ratio, friction angle between the box and particles, and density were established at 6×10^{14} MPa, 0.10, 0.30°, and 5000 kg/m^3, respectively. Secondly, the RMF model, with a length × width of 0.02 m×0.06 m was established (Figure 4b). The mulching film used in Xinjiang is 0.01 mm thick. The thickness of simulated RMF must be within the same order of magnitude as the particle size of soil particles. However, owing to the limited computing resources in the simulation process, the final thickness of the simulated RMF was established at 1 mm, while Young's modulus and Poisson's ratio were set at 10 MPa and 0.1, respectively. The upper and lower parts of the mulching film were filled with soil particles in the box. The Young's modulus, Poisson's ratio, friction angle between the particles, and the density of filled soil particle materials were fixed at 10 MPa, 0.25, 0.2°, and 2400 kg/m^3, respectively. The soil particles were evenly distributed within a range diameter of 0.90-1.10 mm. The simulated soil particle size was 10-fold that of the actual soil particle size, with a total number of filled particles of 15 255 (Figure 4c). The particles were deposited under the action of gravity, which allowed the soil particles and RMF to fall freely to the bottom of the box. Movement, uniform velocity v was first applied to the outermost edge of the RMF model after stabilization of the particle movement, and then the separation force was recorded. The deposition results are shown in Figure 4d.

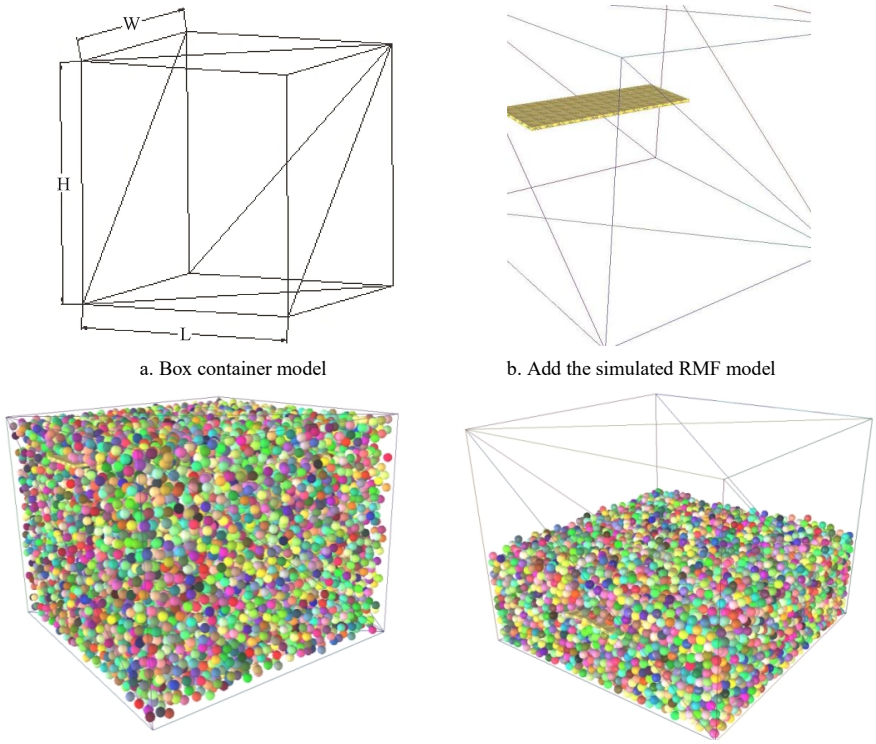

a. Box container model b. Add the simulated RMF model

c. Fill with soil particles d. Gravity deposition

Figure 4 Process of establishing a virtual pull-out model of residual film in the soil

2.3 Separation force experimental design

2.3.1 Equipment equipment and methods

Figure 5 shows the equipment for the RMF-soil separation experiment. Before the experiment, RMF samples that were 0.20 m long, 0.02 m wide, and 0.01 mm thick were cut manually. The lower part of the trough was first uniformly filled with soil before the experiment, and the RMF sample was then spread on the soil in the lower part of the soil trough. One end was extended from the soil trough and clamped using a fixture, while the other end of the fixture was connected to the connecting line. Pulleys were used to connect the tensile force sensor of the universal material mechanical test bench. The soil, which was spread 0.02 m thick on the mulching film tested, was first covered with a plexiglass lid, and the positive pressure on the RMF surface was then adjusted by increasing the weight on lid. Afterward, the universal testbed was started with a speed of the tension sensor of 50 mm/min. The relationship between displacement and the separation force was observed.

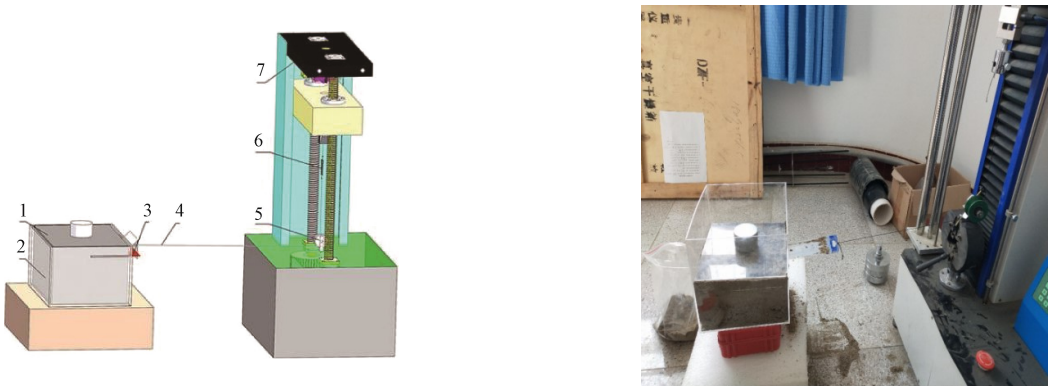

a. RMF- Soil separation test platform model b. Physical photograph of the RMF-soil separation experiment platform

1. Upper part of the soil trough 2. Lower part of the soil trough 3. RMF sample 4. Connecting line 5. Pulley 6. Tension sensor 7. Universal test bench
Note: RMF: Residual mulch film; RMF: residual mulch film.

Figure 5 RMF-soil separation experiment platform model and physical photograph

2.3.2 Single factor experiment design

Experiments on the effect of unused film and used RMF on separation force were performed with unscreened soils. In addition, the positive pressure on the surface of the mulching film was 78 Pa, while the soil moisture content was 8%. The influence of positive pressure on the surface of RMF on the separation force test using unused mulch film and unscreened soil particles with soil moisture of 8% was considered in the experiment. The pressure on the positive surface of RMF was adjusted by increasing the weight above the RMF. The positive surface pressure of RMF was established at five different values, including 74 Pa, 128 Pa, 157 Pa, 186 Pa, and 216 Pa. The effect of soil particle size on the separation force of RMF was tested using unused mulch film and soil with a moisture content of 8%. The soil particle sizes of 5 gradients were established as follows: not screened, <0.6 mm, 0.6-1.6 mm, 1.6-2.5 mm, and >2.5 mm. The effect of soil moisture content on the separation force of RMF was tested using unscreened soil and positive pressure on the surface of RMF of 157 Pa, as well as four gradients of moisture content, namely 0, 8%, 14%, and 19%, were considered. The change in soil moisture

content was determined as follows: the soil was dried first, and different amounts of water were added based on the different contents of soil moisture. The wet soil was sealed and maintained for 24 h to ensure water uniformity in the soil. The factor level table of the single-factor test is listed in Table 3.

Table 3 Factor level comparison table

Factors	Levels				
	0	1	2	3	4
The service life of mulch	Unused film	Used RMF	--	--	--
Normal force/Pa	74	128	157	186	216
Particle size/mm	Not screened	<0.6	0.6-1.6	1.6-2.5	>2.5
Soil moisture content	0%	8%	14%	19%	\

2.3.3 Orthogonal experimental design

In this study, the method of orthogonal combination experiment was used to study the optimal combination of parameters for soil separation with RMF. The orthogonal array was $L_{18}(2^1,3^3)$, with 4 factors that were repeated 18 times. The response index is the maximum separation force of RMF from the soil. The factor level table of the orthogonal factor experiment is listed in Table 4.

Table 4 Factor level comparison table

Factor level	The service life of mulch	Normal force/Pa	Particle size/mm	Soil moisture content
1	Unused film	128	>2.5	0
2	Used RMF	186	1-2.5	8%
3	--	245	<1	14%

3 Results

3.1 Simulation and actual comparison of the experimental results

As shown in Figure 6, with the increase in the separation force, the pull-out displacement of the RMF increased, and the RMF was gradually pulled out. As shown in Figure 7, the simulated separation curve increased rapidly at the beginning of the separation process. The separation force reached a peak value of 5.5 N when the pull-out displacement was 0.03 m. As the pull-out displacement increased, the separation force was again in the downward trend, and the actual separation force curve increased slowly. When the pull-out displacement was 0.06 m, the separation force reached a peak value of 4.5 N and then continued to decline. The separation force decreased after reaching its maximum value, but the simulated separation curve increased rapidly compared with the actual separation force curve and reached the peak separation force first. An analysis of the reasons for this included the preliminary consideration that the thickness of the simulated RMF model is smaller than that of the actual model, and the particle size of the simulated soil is too large. Both the thickness of RMF and the soil particle size will affect the separation force. The actual situation of the simulated separation experiment in the soil is different, and the specific reason merits further study.

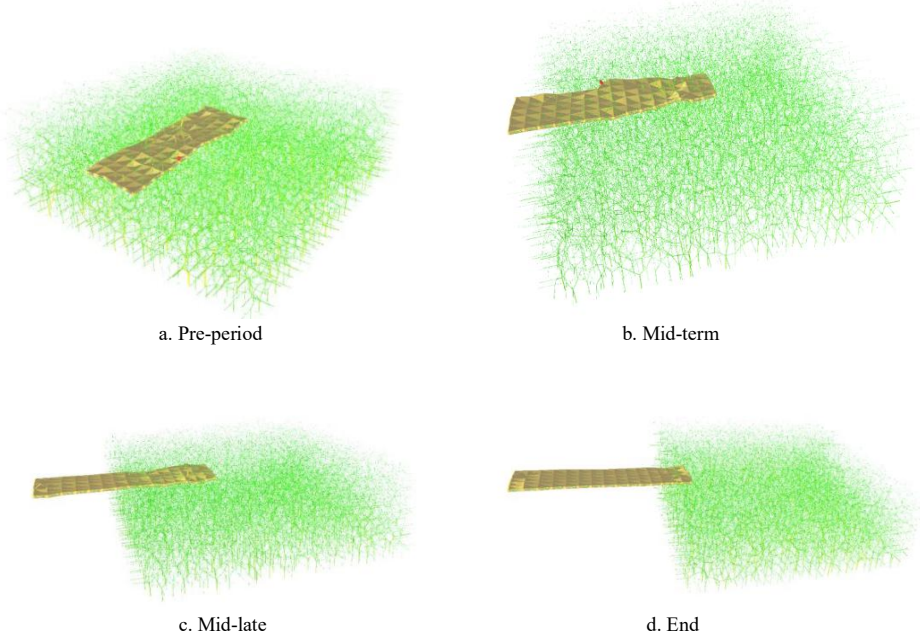

Figure 6 Force chain distribution when the RMF was pulled out in the soil. RMF, residual mulch film

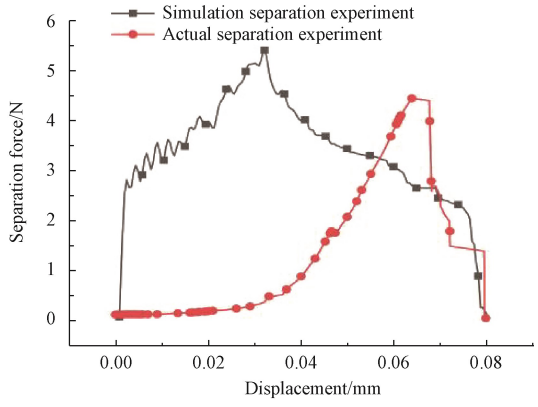

Figure 7 Comparison of simulation and actual separation force of RMF-soil

3.2 Single factor experiment results

3.2.1 Influence of used and unused RMF on separation force

Figure 8 shows that the curve of separation force changed when unused film and used RMF were separated from the soil. The results showed that the maximum separation force values of unused film and used RMF were 1.55 N and 4.34 N, respectively. The separation force of the used RMF was higher than that of the unused film. In addition, by comparing the tensile displacement, it is apparent that the tensile deformation of the used RMF was slightly larger than that of the unused film.

The unused and used mulching films were photographed and observed under a 40× electron microscope (F30-01, WuHan Xingguang Technology Co., Ltd., Wuhan, China). The results are shown in Figure 9. The results revealed that the unused mulching film was smooth and wrinkle-free surface, while the small soil

particles, as well as the wear and wrinkle surface, were observed in the used RMF. This explained the higher separation force obtained by the used RMF.

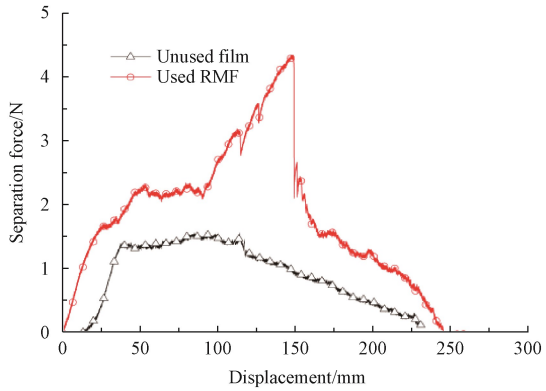

Figure 8 Comparison of the separation force between the unused film and used RMF. RMF, residual mulch film.

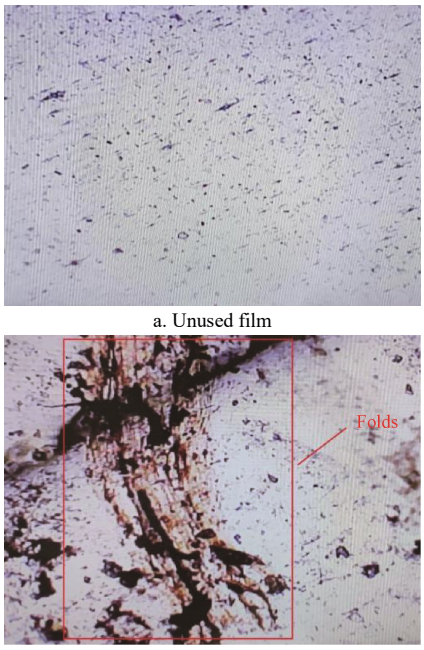

a. Unused film

b. Used RMF

Figure 9 40-fold microscopic view of unused film and used RMF surface

3.2.2 Influence of RMF surface positive pressure on the separation force

The results obtained revealed an upward trend in the variation of the separation force when the RMF was separated from the soil followed by a downward trend (Figure 10). The primary causes of these findings were analyzed in terms of the motion state of the RMF. As the separation force gradually increased, the RMF sample began to elongate, resulting in higher positive pressure and RMF deformation. In addition, at the maximum value of the separation force, the static friction force between the RMF and the soil turns into a dynamic friction force. Simultaneously, as the RMF moves in the soil, the contact area between the mulching film and the soil becomes progressively smaller, thus, resulting in a gradual decrease in the separation force. In summary, the maximum separation force of the RMF gradually increases with increasing positive pressure and tensile elongation. Moreover, increasing the pressure that is exerted on the front of the RMF resulted in a more difficult separation of the RMF from the soil. This continued until the positive pressure value exceeded 216 Pa. This can cause a rupture to occur during the RMF separation process, making the process incapable of separating the RMF from the soil.

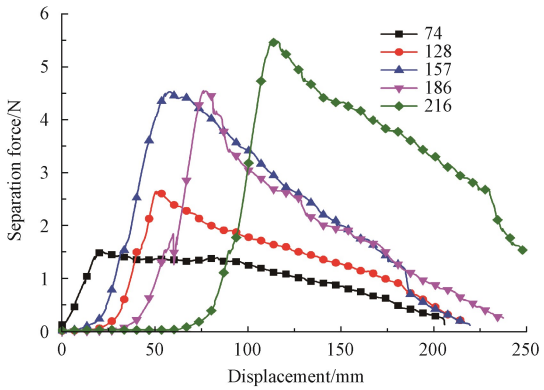

Figure 10 Influence of positive pressure on the surface of RMF on separation force

3.2.3 Influence of soil particle size on the separation force

The influence of soil particle size on the separation force is shown in Figure 11. The results revealed maximal separation force values of 2.667 N, 3.977 N, 4.400 N, and 5.666 N for the particle size ranges of <0.6 mm, 0.6-1.6 mm, 1.6-2.5 mm, and >2.5 mm, respectively, while a maximum separation force of 4.525 N was observed for the unscreened soil. In conclusion, under the same conditions, the separation force of mulching film in the soil increases as the size of soil particles gradually increases.

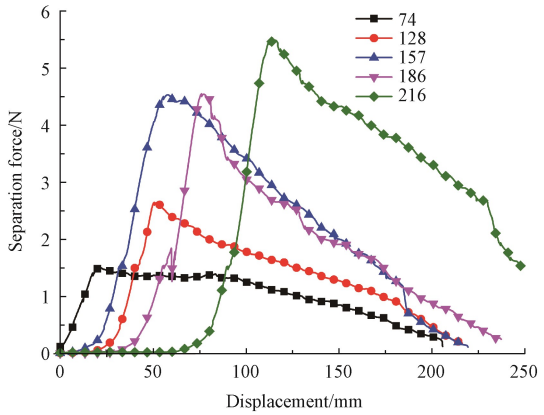

Figure 11 Effect of soil particle size on separation force

Based on the established RMF-soil simulation contact model, this analysis shows that when the RMF and soil are in contact with each other, the RMF will be deformed by the extrusion of soil particles. Figure 12 shows that the torsional and bending deformation of the RMF surface occurred after deformation. The results indicated significant RMF deformation at larger sizes of soil particles, Moreover, the force of action of the soil particles as the RMF was pulled out gradually changed from tangential friction to normal resistance, thus, suggesting that a larger particle diameter results in a greater separation force.

3.2.4 Influence of soil moisture content on the separation force

Figure 13 shows the influence of soil moisture content on the separation force of residual film in the soil. The results showed that the maximum separation force of residual film values were 5.552, 3.717, 4.278, and 7.854 N at soil moisture contents of 0, 8%, 14%, and 19%, respectively. However, a soil moisture content greater than 19% makes the soil waterlogged. Thus, the mulching film could not be pulled out from the soil.

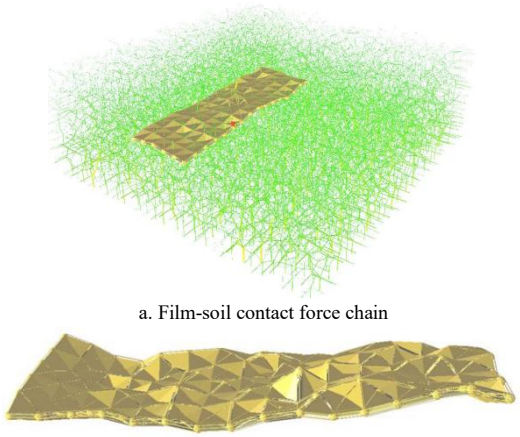

a. Film-soil contact force chain

b. Simulated residual film after contact deformation

Figure 12 Contact deformation of the mulch film-soil

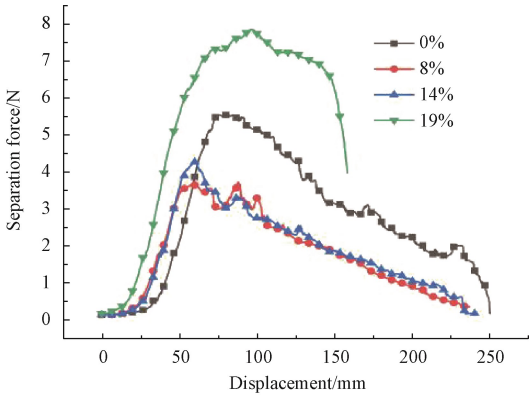

Figure 13 Effect of water content on the separation force

In conclusion, with the increase in the content of soil moisture, the maximum separation force of RMF in the soil showed a trend of decreasing first and then increasing at very high or very low moisture contents. This could further complicate the separation of the RMF from the soil. However, a soil moisture content of approximately 8% was the most effective at facilitating the separation and recovery of the RMF from the soil. These findings can be explained by the fact that low contents of soil moisture result in a high friction coefficient between the soil and RMF. Thus, a high separation force is required to effectively remove the film residue. In contrast, when the soil has a high content of soil moisture, the soil water exerts a high force on the RMF, which results in a high separation force.

3.3 Orthogonal experimental results

The importance of parameters in the influence of the separation force of RMF in soil was ranked as shown in Table 5.

The order of importance from the highest to lowest was particle diameter, positive pressure on the surface of the RMF, soil moisture content, and the length of time that the RMF was used. The most optimal parameter combination for the separation of film residue from the soil was A2, B1, C1, and D2, which refers to a used RMF, a pressure value on the front of an RMF of 128 Pa, the soil particle size of over 2.5 mm, and a soil moisture content of 8%. The positive pressure on the surface of the RMF can be equivalent to the gravity of the soil directly above the RMF sample when the pressure on the front of the RMF was 128 Pa, and the RMF was buried at approximately 60 mm. Therefore, burying the mulch 60 mm deep in soil that has particle sizes over 25 mm and a moisture content of 8% is the optimal combination of parameters to effectively separate the film mulching residue from the soil.

Table 5 Results of the orthogonal experiment

Test number	Used and unused A	Positive pressure B	Particle size C	Moisture content D	Maximum separation force/N
1	1	1	1	1	2.98
2	1	1	2	2	3.41
3	1	1	3	3	8.10
4	1	2	1	1	3.83
5	1	2	2	2	4.85
6	1	2	3	3	9.77
7	1	3	1	2	3.61
8	1	3	2	3	6.31
9	1	3	3	1	11.62
10	2	1	1	3	2.49
11	2	1	2	1	2.70
12	2	1	3	2	7.46
13	2	2	1	2	2.64
14	2	2	2	3	3.57
15	2	2	3	1	7.56
16	2	3	1	3	5.47
17	2	3	2	1	6.53
18	2	3	3	2	7.93
K1	54.50	27.14	21.02	35.23	
K2	46.34	32.22	27.37	29.90	
K3		41.48	52.46	35.70	
k1	6.05	4.52	3.50	5.87	
k2	5.15	5.37	4.56	4.98	
k3		6.91	8.74	5.95	
Range R	0.90	2.39	5.24	0.97	
Primary and secondary order			C>B>D>A		
Excellent level	A2	B1	C1	D2	
Excellent combination			A2, B1, C1, D2		

4 Discussion

4.1 Simulation and actual separation experiment results and analysis

This study established an RMF-soil contact constitutive model with DEM and used the established constitutive model to simulate the process of separating the RMF and soil. A comparison of the RMF-soil simulation with the actual separation force indicated that the morphological characteristics of the two are basically the same, but they differ significantly in their force-displacement. This may be due to the deviation of the soil particle size and RMF thickness of the simulated model from the actual soil particle size and RMF thickness. It is expected that other researchers will develop more advanced methods to simulate and build a more accurate contact model in the future.

4.2 Analysis of the single factor experimental results

The single factor experiment showed that the separation force of the used RMF was higher than that of the unused mulching film. Under the same conditions, the maximum separation force required to separate the RMF was proportional to positive pressure on the surface of RMF and the size of the soil particles. As the positive pressure on the RMF surface increased, the separation force gradually increased. As the soil particle sizes increase, the separation force increases. Under the same conditions, the maximum separation force required to separate the RMF was proportional to the positive pressure on the surface of RMF and the size of the soil particle size. With an increase in the soil moisture content, the maximum separation force decreased first and then increased. This led us to hypothesize that a high content of soil moisture leads to a water film in the soil that has a large force on RMF, thus, resulting in a large separation force.

4.3 Analysis of the orthogonal experiment results

The orthogonal experiment results showed that the soil particle size had the greatest effect on the maximum separation force, followed by positive pressure on the RMF surface, soil moisture content, and service life of RMF. In summary, burying the film mulch 60 mm deep in soil that has particle sizes greater than 2.5 mm and a soil moisture content of 8% was the optimal combination of parameters to effectively separate the film mulching residue from the soil.

4.4 Outlook

1) The RMF-soil contact constitutive model established in this paper is a linear model, and there is adhesion between the soil and contact objects; the adhesion is a complex interface behavior[38]. The interfacial adhesion between the RMF and soil is also an important factor that affects the separation of RMF and soil. In the future, a viscoplastic RMF-soil contact constitutive model can be tried to establish[39].

2) The contact behavior of the RMF and soil is complex, and the contact force between the RMF and soil involves many factors. In addition, there are complex interactions among the factors. This paper only explored the effects of soil particle size, soil moisture content, unused film, used RMF, and positive pressure on the RMF surface on the RMF-soil separation force. Other influencing factors can be considered in the future, including film properties, soil bulk density, soil texture, and soil compaction among others.

5 Conclusions

The goal of this study was to investigate the separation mechanism of RMF in topsoil and determine the conditions conducive to its separation. A constitutive model of RMF-soil particle contact was established based on the DEM, and the separation of RMF and soil was simulated. The effects of various factors on the RMF-soil separation force were studied by single-factor and orthogonal experiments, and the most favorable combination of parameters for the RMF-soil separation was determined. A comparison of the RMF-soil simulation with the actual separation force showed that the morphological characteristics of the two were basically the same, but they differed significantly in forced displacement. This may be due to the deviation of the soil particle size and RMF thickness of the simulated model from the actual soil particle size and RMF thickness. It is expected that other researchers will develop more advanced methods to simulate and establish a more accurate contact model in the future. This study will help to explore the mechanism of separation between RMF and soil and the regulation of RMF.

Acknowledgements

This work was financially supported by the Support Plan for the National Natural Science Foundation of China (Grant No. 32060288), and the National Natural Science Foundation of China (Grant No. 32160300) for supporting this research. The authors are grateful to anonymous reviewers for their comments.

[References]

[1] Gao W H, Han R. Xinjiang Statistical Yearbook-2021. Beijing: China Statistics Press, 2021; 321–326. (in Chinese)

[2] Li W M, Wang H S. China Xinjiang Production and Construction Corps Statistical Yearbook. Beijing: Statistics Press, 2021; pp.181–183. (in Chinese)

[3] Luo L C, Hui X L, He G, Wang S, Wang Z H, Siddique K H M. Benefits and limitations to plastic mulching and nitrogen fertilization on grain yield and sulfur nutrition: multi-site field trials in the semiarid area of China. Frontiers in Plant Science, 2022; 13(13): 799093. doi: 10.3389/fpls.2022.799093.

[4] Li Y, Zhang Z X, Wang J W, Zhang M Z. Soil aeration and plastic film mulching increase the yield potential and quality of tomato (*Solanum lycopersicum*). Agriculture, 2022; 12(2): 269–269.

[5] Liao Z Q, Zhang K B, Fan J L, Li Z J, Zhang F C, Wang X K, et al. Ridge-furrow plastic mulching and dense planting with reduced nitrogen improve soil hydrothermal conditions, rainfed soybean yield and economic return in a semi-humid drought-prone region of China. Soil and Tillage Research, 2022; 217: 105291. doi: 10.1016/j.still.2021.105291.

[6] Hu Z E, Xiao M L, Wang S, Tong Y Y, Lu S B, Chen J P, et al. Effects of plastic mulch film on soil nutrients and ecological enzyme stoichiometry in farmland. Environmental Science, 2022; 43(3): 1649–1656. (in Chinese)

[7] Ferreira-Filipe D A, Paco A, Natal-da-Luz T, Sousa J P, Saraiva J A, Duarte A C, et al. Are mulch biofilms used in agriculture an environmentally friendly solution? - An insight into their biodegradability and ecotoxicity using key organisms in soil ecosystems. Science of The Total Environment, 2022; 828: 154269. doi: 10.1016/j.scitotenv.2022.154269.

[8] Liang R Q, Chen X G, Zhang B C, Meng H W, Jiang P, Peng X B, et al. Problems and countermeasures of recycling methods and resource reuse of residual film in cotton fields of Xinjiang. Transactions of the CSAE, 2019; 35(16): 1–13. (in Chinese)

[9] Wang S Y, Fan T L, Cheng W L, Wang L, Zhao G, Li S Z, et al. Occurrence of macroplastic debris in the long-term plastic film-mulched agricultural soil: A case study of Northwest China. Sci Total Environ, 2022; 831: 154881. doi: 10.1016/j.scitotenv.2022.154881.

[10] Tian X, Yang M N, Guo Z L, Chang C P, Li J F, Gua Z X, et al. Plastic mulch film induced soil microplastic enrichment and its impact on wind-blown sand and dust. Science of The Total Environment, 2021; 813: 152490. doi: 10.1016/j.scitotenv.2021.152490.

[11] Li S T, Ding F, Flury M, Wang Z, Xu L, Li S Y, et al. Macro- and

microplastic accumulation in soil after 32 years of plastic film mulching. Environmental Pollution, 2022; 300: 118945. doi: 10.1016/j.envpol.2022.118945.

[12] He W Q, Yan C R, Zhao C X, Chang R Q, Liu Q, Liu S. Study on the pollution by plastic mulch film and its countermeasures in China. Journal of Agro-Environment Science, 2009; 28(3): 533–538. (in Chinese)

[13] Hu C, Wang X F, Wang S G, Lu B, Guo W S, Liu C J, et al. Impact of agricultural residual plastic film on the growth and yield of drip-irrigated cotton in arid region of Xinjiang, China. Int J Agric & Biol Eng, 2020; 13(1): 160–169.

[14] Wang D W, Wang Z H, Ding H W, Zhou B, Zhang J Z, Li W H, et al. Effects of biodegradable mulching films on soil hydrothermal conditions and yield of drip-irrigated cotton (*Gossypium hirsutum* L.). Int J Agric & Biol Eng, 2022; 15(6): 153–164.

[15] Liang R Q, Chen X G, Jiang P, Zhang B C, Meng H W, Peng X B, et al. Calibration of the simulation parameters of the particulate materials in film mixed materials. Int J Agric & Biol Eng, 2020; 13(4): 29–36.

[16] Zhang W W, Wang L H, Zhou J Q, Zhu K L, Sun S J. Degradability of biodegradable plastic films and its mulching effects on soil temperature and maize yield in northeastern China. Int J Agric & Biol Eng, 2020; 13(2): 146–153.

[17] Xu R L, Hai R T. Effect of plastic plastic film on wheat seed germination and seedling antioxidant enzyme system. Ecology and Environmental Sciences, 2010; 19(11): 2702–2707. (in Chinese)

[18] Qi Y L, Ossowicki A, Yang X M, Huerta Lwanga E, Dini-Andreote F, Geissen V, et al. Effects of plastic mulch film residues on wheat rhizosphere and soil properties. Journal of Hazardous Materials, 2020; 387: 121711. doi: 10.1016/j.jhazmat.2019.121711.

[19] Gao W C, Cai K, Zeng Y T, Lin Y C, Wu S, Luo X B, et al. Impacts of mulching plastic film residue on migration of soil nitrogen and growth of flue-cured tobacco roots. Acta Pedologica Sinica, 2020; 57(6): 1556–1563. (in Chinese)

[20] Li Y Q, Zhao C X, Yan C R, Mao L L, Liu Q, Li Z, et al. Effects of agricultural plastic film residues on transportation and distribution of water and nitrate in soil. Chemosphere, 2020; 242(C): 125–131.

[21] Liu Y, Huang Q, Hu W, Qin J M, Zheng X R, Wang J F, et al. Effects of plastic mulch film residues on soil-microbe-plant systems under different soil pH conditions. Chemosphere, 2021; 26: 128901. doi: 10.1016/j.chemosphere.2020.128901.

[22] Wang X L, Hu H, Wang Q J, Li H W, He J, Chen W Z. Calibration method of soil contact characteristic parameters based on DEM theory. Transactions of the CSAM, 2017; 48(12): 78–85. (in Chinese)

[23] Lobo-Guerrero S, Vallejo L E. Fiber-reinforcement of granular materials: Dem visualization and analysis. Geomech. Geoengin, 2010; 5(2): 79–89.

[24] Villard P, Chevalier B, Hello B L, Combe G. Coupling between finite and discrete element methods for the modelling of earth structures reinforced by geosynthetic. Compute. Geotech, 2009; 36(5): 709–717

[25] Tran V, Meguid M, Chouinard L. A finite-discrete element framework for the 3D modeling of geogride soil interaction under pullout loading conditions. Geotext. Geomembr, 2013; 37: 1–9.

[26] O-nate E, Rojek J. Combination of discrete element and finite element methods for dynamic analysis of geomechanics problems. Computer Methods in Applied Mechanics and Engineering, 2004; 193(27): 3087–3128.

[27] Effeindzourou A, Chareyre B, Thoeni K, Giacomini A, Kneib F. Modelling of deformable structures in the general framework of the discrete element method. Geotextiles and Geomembranes, 2016; 44(2): 143–156.

[28] Thoeni K, Effeindzourou A, Chareyre B, Giacomini A. Discrete modelling of soil-Inclusion problems. Applied Mechanics and Materials, 2016; 4097(846): 397–402.

[29] de Gennes P G. Granular matter: A tentative view. In: More things in heaven and earth, Springer, 1999; pp.629–643.

[30] Dong Y X, Song Z P, Cui S J. Perspectives on the measurement of angle of repose. Journal of China Pharmaceutical University, 2008; 39(4): 317–320. (in Chinese)

[31] Smilauer V, Angelidakis V, Catalano E, Caulk R, Chareyre B, Chèvremont W, et al. Yade Documentation (3rd ed). The Yade Project, 2021.

[32] Peña A A, Lizcano A, Alonso-Marroquin F, Herrmann H J. Biaxial test simulations using a packing of polygonal particles. International Journal Numerical and Analytical Methods in Geomechanics, 2008; 32(2): 143–160.

[33] Alonso-Marroquín F, Wang C Y. An efficient algorithm for granular dynamics simulations with complex-shaped objects. Granular Matter, 2009; 11(5): 317–329.

[34] Lu G, Third J R, Müller C R. Discrete element models for non-spherical particle systems: From theoretical developments to applications. Chemical Engineering Science, 2015; 127: 425–465.

[35] Campen M, Kobbelt L. Polygonal boundary evaluation of minkowski sums and swept volumes. Computer Graphics Forum, 2010; 29(5): 1613–1622.

[36] Peternell M, Steiner T. Minkowski sum boundary surfaces of 3D-objects. Graphical Models, 2007; 69(3-4): 180–190.

[37] Zeng Z W, Ma X, Cao X L, Li Z H, Wang X C. Critical review of applications of discrete element method in agricultural engineering. Transactions of the CSAM, 2021; 52(4): 1–20. (in Chinese)

[38] Zhou Y C, Wright B D, Yang R Y, Xu B H, Yu A B. Rolling friction in the dynamic simulation of sandpile formation. Physica A: Statistical Mechanics and its Applications, 1999; 269(2): 536–553.

[39] Oda M, Iwashita K. Study on couple stress and shear band development in granular media based on numerical simulation analyses. International Journal of Engineering Science, 2000; 38(15): 1713–1740.